Mimetic finite difference methods for diffusion equations on non-orthogonal AMR meshes

Konstantin Lipnikov Jim Morel Mikhail Shashkov

Los Alamos National Laboratory
T-7 & CCS-4, MS B284, Los Alamos, NM 87545
lipnikov@lanl.gov, jim@lanl.gov, shashkov@lanl.gov

Contents

- Objectives
- Local support operator method
- Mimetic discretizations on locally refined meshes
- Numerical experiments
- Comparison with other discretization methods
- Conclusions

Objectives

What are the perfect discretizations?

- they preserve and mimic mathematical properties of physical systems;
- they are accurate on adaptive smooth and non-smooth grids;

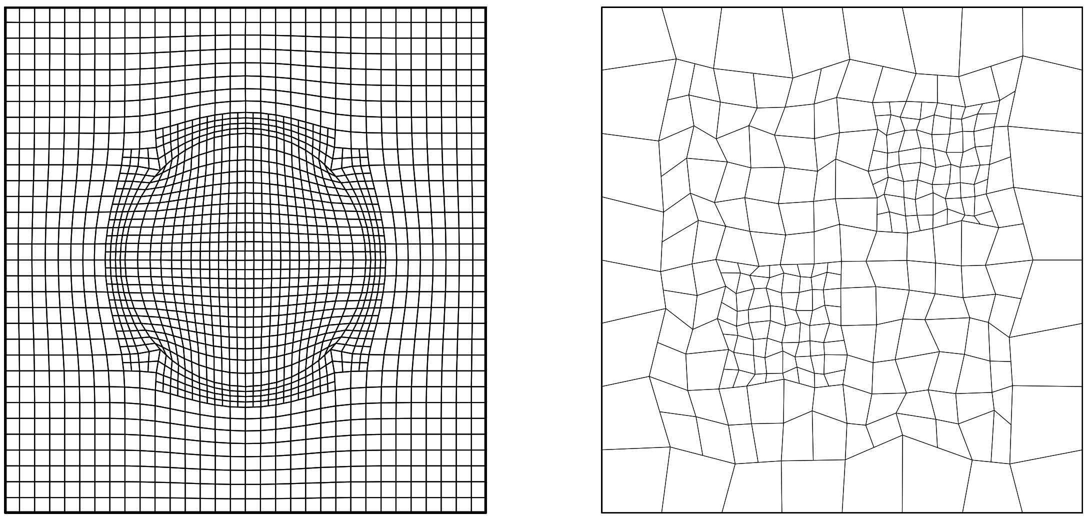

Objectives

What are the perfect discretizations?

- they preserve and mimic mathematical properties of physical systems;
- they are accurate on adaptive smooth and non-smooth grids;
- they can be used for a wide family of grids and operators.

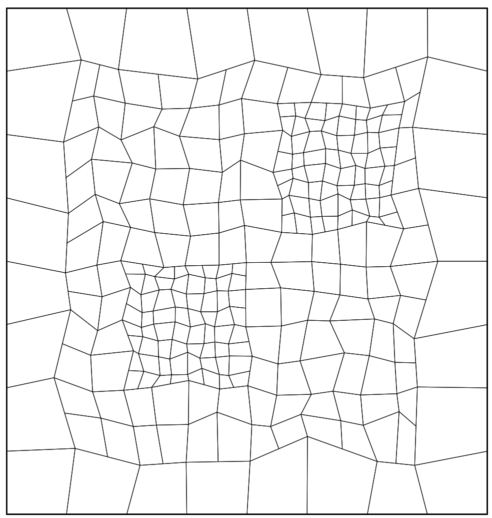

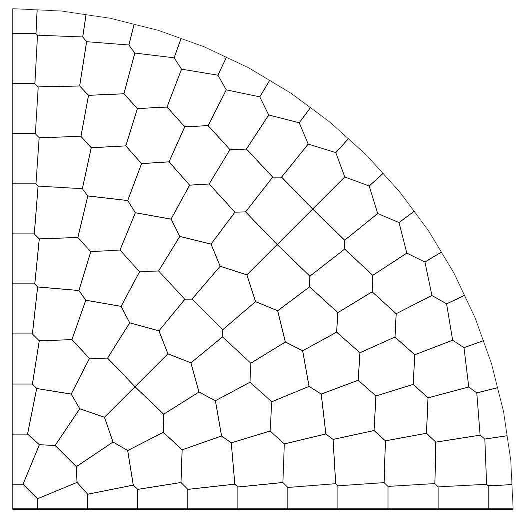

Los Alamos NATIONAL LABORATORY

Model diffusion problem

We consider the elliptic equation

$$-\mathrm{div}(\boldsymbol{K}\,\nabla p) = b \qquad \text{in} \qquad \Omega$$

subject to the homogeneous Dirichlet b.c.

$$p = 0 \qquad \text{on} \qquad \partial\Omega.$$

The problem can be reformulated as a system of first order equations:

$$\begin{aligned} \mathrm{div}\,\boldsymbol{f} &= b, \\ \boldsymbol{f} &= -\boldsymbol{K}\,\nabla p. \end{aligned}$$

For simplicity we assume that $\boldsymbol{K} = \boldsymbol{I}$.

Support operator method (1/2)

Consider the mathematical identity:

$$\int_e \boldsymbol{f} \cdot \mathrm{grad} p \, \mathrm{d}x + \int_e \mathrm{div} \, \boldsymbol{f} \, p \, \mathrm{d}x = \int_{\partial e} p \, \boldsymbol{f} \cdot \boldsymbol{n} \, \mathrm{d}l.$$

Local support-operators (SO) methodology (for div & grad):

1. define degrees of freedom for variables p and $\boldsymbol{f}$;
2. discretize the identity using accurate quadrature rules;
3. choose a discrete approximation to the divergence operator, the *prime* operator DIV;
4. derive the discrete approximation of the gradient operator, the *derived* operator GRAD, from the discrete Green formula:

$$[f^d, \, \mathrm{GRAD} \, p^d]_X = -[\mathrm{DIV} \, f^d, \, p^d]_Q + < p^d, \, f^d >_L \qquad \forall f^d, p^d.$$

Support operator method (1/2)

Consider the mathematical identity:

$$\int_e \boldsymbol{f} \cdot \mathrm{grad} p \, \mathrm{d}x + \int_e \mathrm{div} \, \boldsymbol{f} \, p \, \mathrm{d}x = \int_{\partial e} p \, \boldsymbol{f} \cdot \boldsymbol{n} \, \mathrm{d}l.$$

Local support-operators (SO) methodology (for div & grad):

1. define degrees of freedom for variables p and $\boldsymbol{f}$;
2. discretize the identity using accurate quadrature rules;
3. choose a discrete approximation to the divergence operator, the *prime* operator DIV;
4. derive the discrete approximation of the gradient operator, the *derived* operator GRAD, from the discrete Green formula:

$$[f^d, \, \mathrm{GRAD} \, p^d]_X = -[\mathrm{DIV} \, f^d, \, p^d]_Q + < p^d, \, f^d >_L \qquad \forall f^d, p^d.$$

Support operator method (2/2)

Applications of the SO methodology include:

- Electromagnetics: discrete operators DIV, $\overline{\text{GRAD}}$, CURL and $\overline{\text{CURL}}$ mimic:

$$\operatorname{div}\operatorname{curl} = 0, \qquad \operatorname{curl}\operatorname{grad} = 0$$

$$\int_e \operatorname{curl}\boldsymbol{E} \cdot \boldsymbol{H}\,\mathrm{d}x = \int_e \operatorname{curl}\boldsymbol{H} \cdot \boldsymbol{E}\,\mathrm{d}x + \oint_{\partial e} (\boldsymbol{E} \times \boldsymbol{H}) \cdot \boldsymbol{n}\,\mathrm{d}l$$

- CFD: discrete operators DIV and GRAD mimic:

$$\int_e \operatorname{grad}\boldsymbol{u} : \boldsymbol{T}\,\mathrm{d}x = -\int_e \operatorname{div}\boldsymbol{T} \cdot \boldsymbol{u}\,\mathrm{d}x + \oint_{\partial e} \boldsymbol{u} \cdot (\boldsymbol{T} \cdot \boldsymbol{n})\,\mathrm{d}l$$

- Gas dynamics, poroelasticity, magnetic diffusion, radiation diffusion, etc...

Mimetic discretizations (1/8)

Step 1 (degrees of freedom for p and $\boldsymbol{f}$).

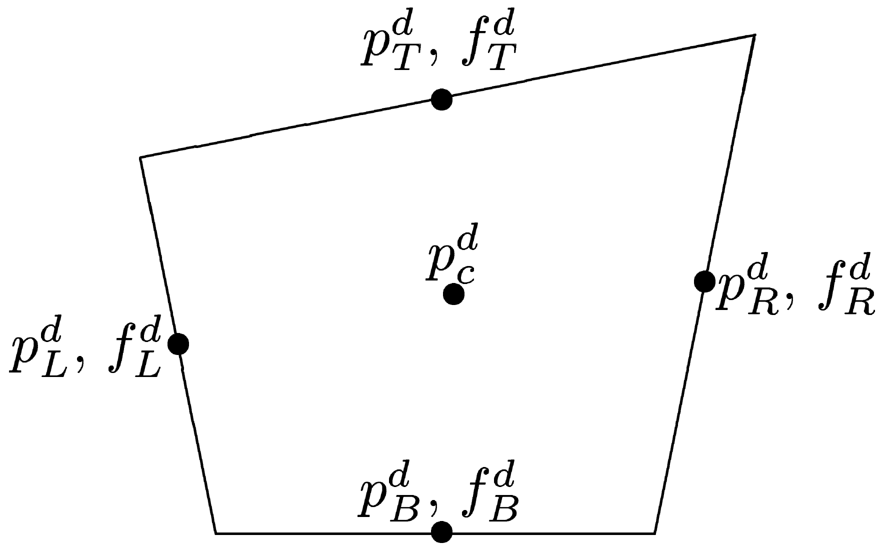

- $p_c^d, p_B^d, \ldots, p_L^d$ are defined at the cell center and edge mid-points.
- $f_B^d, \ldots, f_L^d$ are defined at mid-points of cell edges. They approximate the normal components of $\boldsymbol{f}$, e.g.

$$f_L^d \approx \boldsymbol{f} \cdot \boldsymbol{n}_L.$$

Mimetic discretizations (2/8)

Steps 2 (discrete identity).

- $$\int_e \mathrm{div}\,\boldsymbol{f}\,p\,\mathrm{d}x \approx (\mathrm{DIV}\,f^d)_c\,p^d_c\,|e|$$
- $$\int_{\partial e} p\,\boldsymbol{f}\cdot\boldsymbol{n}\,\mathrm{d}l \approx p^d_R f^d_R |l_R| + p^d_T f^d_T |l_T| + p^d_L f^d_L |l_L| + p^d_B f^d_B |l_B|$$
- $$\int_e \boldsymbol{f}\cdot\mathrm{grad}p\,\mathrm{d}x \approx [f^d,\,\mathrm{GRAD}\,p^d]_{X_e}$$

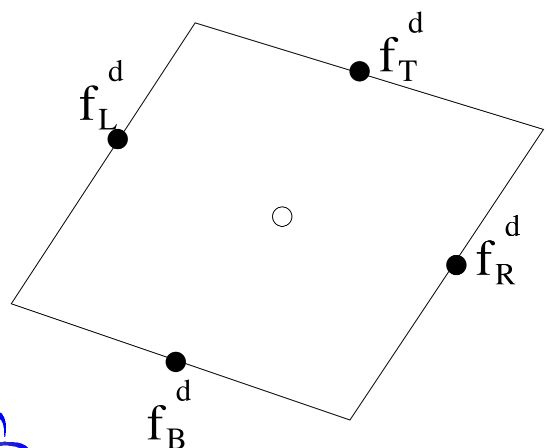

The vectors can be recovered uniquely at four vertices of quadrilateral e. Let

$$[f^d,\,g^d]_{X_e} = \frac{1}{2}\sum_{j=1}^{4} |T_j|\,\boldsymbol{f}^d_j\cdot\boldsymbol{g}^d_j$$

Mimetic discretizations (2/8)

Steps 2 (discrete identity).

- $$\int_e \mathrm{div}\,\boldsymbol{f}\, p\, \mathrm{d}x \approx (\mathrm{DIV}\; f^d)_c\, p_c^d\, |e|$$
- $$\int_{\partial e} p\, \boldsymbol{f} \cdot \boldsymbol{n}\, \mathrm{d}l \approx p_R^d f_R^d |l_R| + p_T^d f_T^d |l_T| + p_L^d f_L^d |l_L| + p_B^d f_B^d |l_B|$$
- $$\int_e \boldsymbol{f} \cdot \mathrm{grad} p\, \mathrm{d}x \approx [f^d,\, \mathrm{GRAD}\, p^d]_{X_e}$$

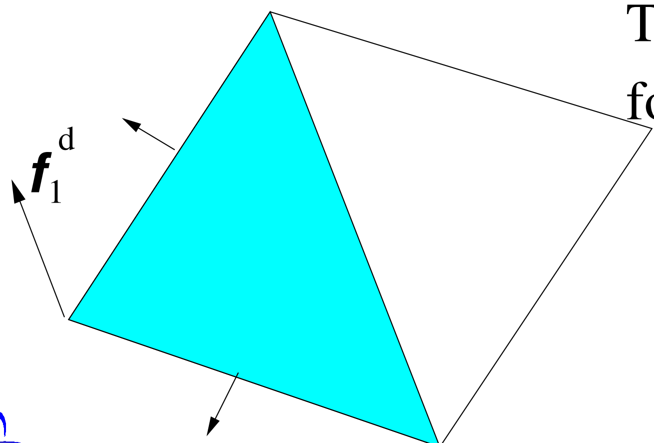

The vectors can be recovered uniquely at four vertices of quadrilateral e. Let

$$[f^d,\, g^d]_{X_e} = \frac{1}{2} \sum_{j=1}^{4} |T_j|\, \boldsymbol{f}_j^d \cdot \boldsymbol{g}_j^d$$

Mimetic discretizations (2/8)

Steps 2 (discrete identity).

- $$\int_e \mathrm{div}\, \boldsymbol{f}\, p\, \mathrm{d}x \approx (\mathrm{DIV}\, f^d)_c\, p_c^d\, |e|$$
- $$\int_{\partial e} p\, \boldsymbol{f} \cdot \boldsymbol{n}\, \mathrm{d}l \approx p_R^d f_R^d |l_R| + p_T^d f_T^d |l_T| + p_L^d f_L^d |l_L| + p_B^d f_B^d |l_B|$$
- $$\int_e \boldsymbol{f} \cdot \mathrm{grad} p\, \mathrm{d}x \approx [f^d,\, \mathrm{GRAD}\, p^d]_{X_e}$$

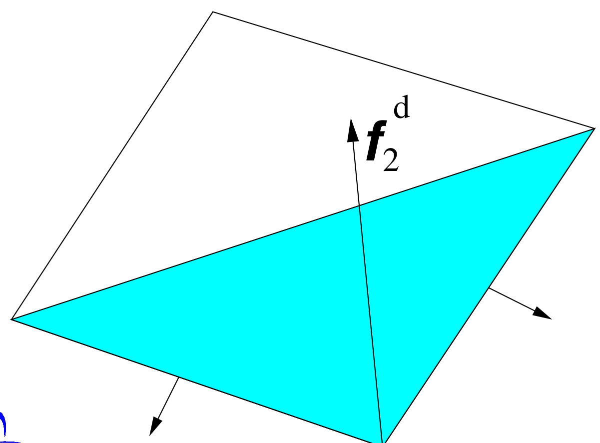

The vectors can be recovered uniquely at four vertices of quadrilateral e. Let

$$[f^d,\, g^d]_{X_e} = \frac{1}{2} \sum_{j=1}^{4} |T_j|\, \boldsymbol{f}_j^d \cdot \boldsymbol{g}_j^d$$

Mimetic discretizations (2/8)

Steps 2 (discrete identity).

- $$\int_e \operatorname{div} \boldsymbol{f}\, p \,\mathrm{d}x \approx (\mathrm{DIV}\, f^d)_c\, p_c^d\, |e|$$
- $$\int_{\partial e} p\, \boldsymbol{f} \cdot \boldsymbol{n} \,\mathrm{d}l \approx p_R^d f_R^d |l_R| + p_T^d f_T^d |l_T| + p_L^d f_L^d |l_L| + p_B^d f_B^d |l_B|$$
- $$\int_e \boldsymbol{f} \cdot \operatorname{grad} p \,\mathrm{d}x \approx [f^d,\, \mathrm{GRAD}\, p^d]_{X_e}$$

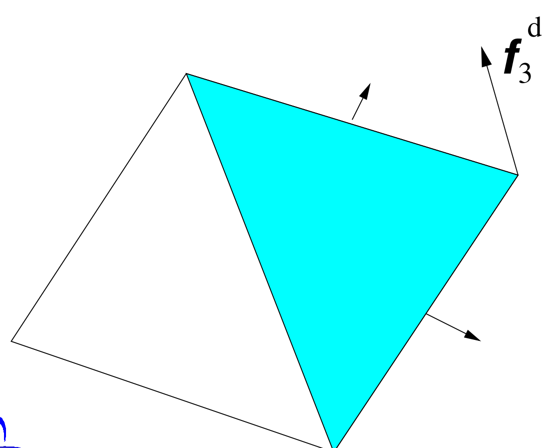

The vectors can be recovered uniquely at four vertices of quadrilateral e. Let

$$[f^d,\, g^d]_{X_e} = \frac{1}{2} \sum_{j=1}^{4} |T_j|\, \boldsymbol{f}_j^d \cdot \boldsymbol{g}_j^d$$

Mimetic discretizations (3/8)

Steps 3 (prime operator).

The prime operator DIV follows from the Gauss theorem:

$$\operatorname{div} \boldsymbol{f} = \lim_{|e|\to 0} \frac{1}{|e|} \oint_{\partial e} \boldsymbol{f} \cdot \boldsymbol{n}\, dl.$$

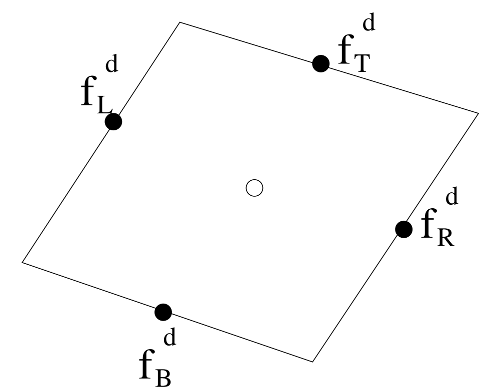

Center-point quadrature gives

$$(\mathrm{DIV}\ f^d)_c = \frac{1}{|e|} \left(f_R^d |l_R| + f_T^d |l_T| + f_L^d |l_L| + f_B^d |l_B| \right).$$

Mimetic discretizations (4/8)

Step 4 (derived operator).

Replacing integrals in the Green formula by their approximations, we get

$$\mathrm{GRAD}\, p^d = \mathcal{M}_e^{-1} \begin{pmatrix} |l_R|(p_R^d - p_c^d) \\ |l_T|(p_T^d - p_c^d) \\ |l_L|(p_L^d - p_c^d) \\ |l_B|(p_B^d - p_c^d) \end{pmatrix}$$

where

$$< \mathcal{M}_e f^d,\, g^d >= [f^d,\, g^d]_{X_e}$$

and $f^d = (f_R^d, f_T^d, f_L^d, f_B^d)^t$. The local discretization reads

$$\begin{aligned} \mathrm{DIV}\, f^d &= b^d, \\ f^d &= -\mathrm{GRAD}\, p^d. \end{aligned}$$

Mimetic discretizations (5/8)

Short summary.

- matrix $M_e^{-1} \in \Re^{4\times 4}$;
- discrete divergence and gradient operators mimic essential properties of the continuous operators (local mass conservation, Green formula);
- discretization and continuity conditions are separated;
- we do not assume anything about a grid structure, i.e. the discretization method is applicable to both conformal and non-conformal meshes.

Mimetic discretizations (6/8)

$$\int_{\partial e} p\,\boldsymbol{f} \cdot \boldsymbol{n}\,\mathrm{d}l \approx p_R^d f_R^d |l_R| + p_T^d f_T^d |l_T| + p_L^d f_L^d |l_L| + p_B^d f_B^d |l_B|.$$

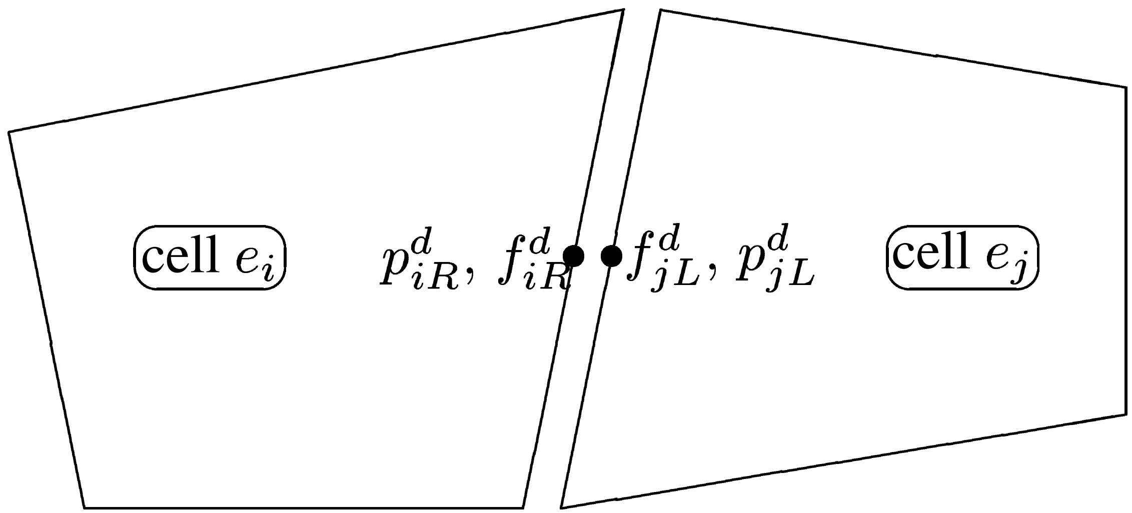

The global discretization is achieved by imposing the continuity of fluxes

$$f_{iR}^d = -f_{jL}^d$$

and interface intensities

$$p_{iR}^d = p_{jL}^d.$$

Mimetic discretizations (6/8)

$$p^d_{iR} f^d_{iR} + p^d_{jL} f^d_{jL} = 0.$$

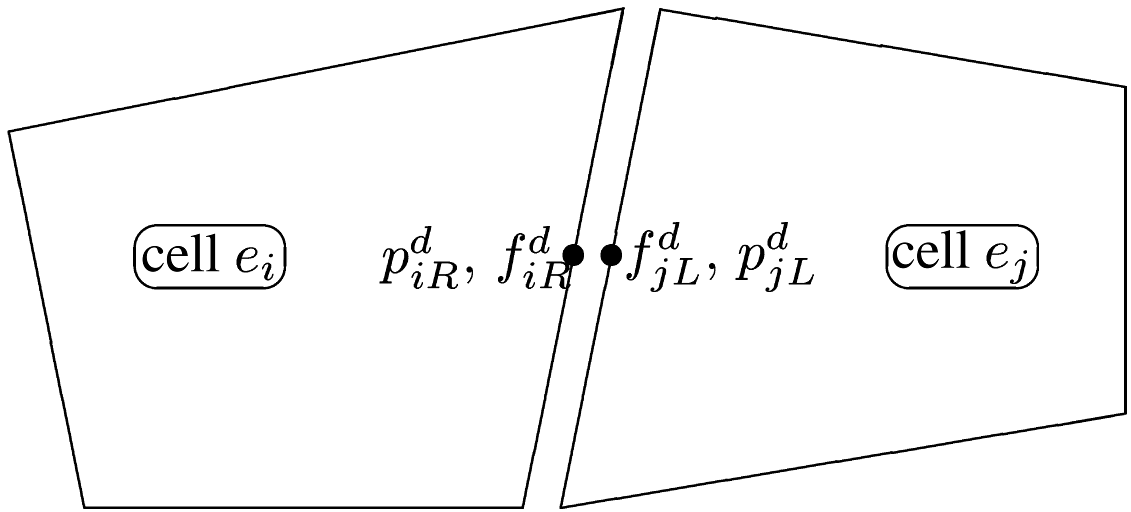

The global discretization is achieved by imposing the continuity of fluxes

$$f^d_{iR} = -f^d_{jL}$$

and interface intensities

$$p^d_{iR} = p^d_{jL}.$$

Mimetic discretizations (7/8)

$$p_{iR}^d f_{iR}^d + p_{jL}^d f_{jL}^d + p_{kL}^d f_{kL}^d = 0.$$

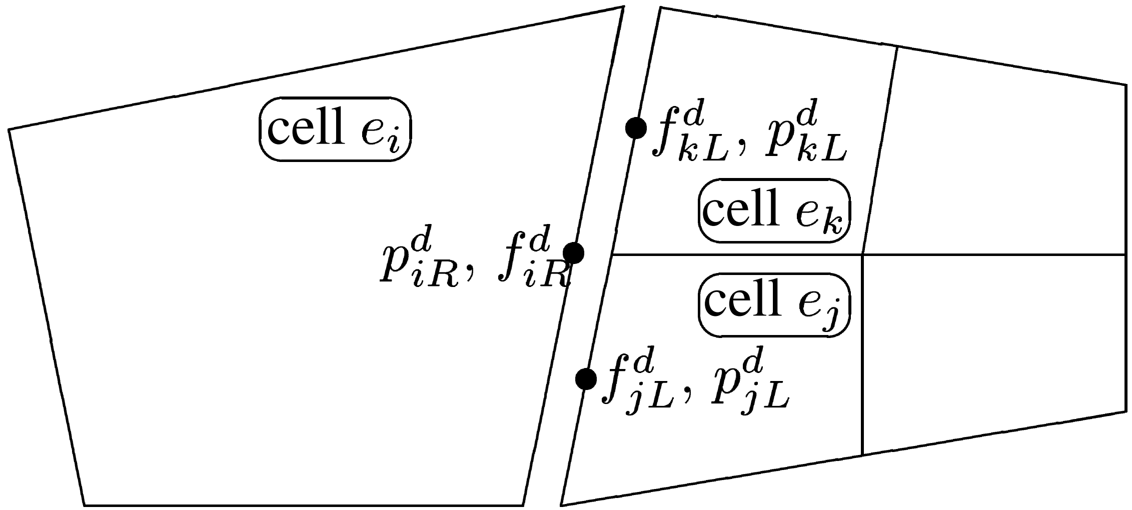

The global discretization is achieved by imposing the continuity of fluxes

$$f_{iR}^d = -f_{jL}^d = -f_{kL}^d$$

and interface intensities

$$|l_{iR}|\, p_{iR}^d = |l_{jL}|\, p_{jL}^d + |l_{kL}|\, p_{kL}^d.$$

Mimetic discretizations (8/8)

Stencils of a stiffness matrix for interface intensities.

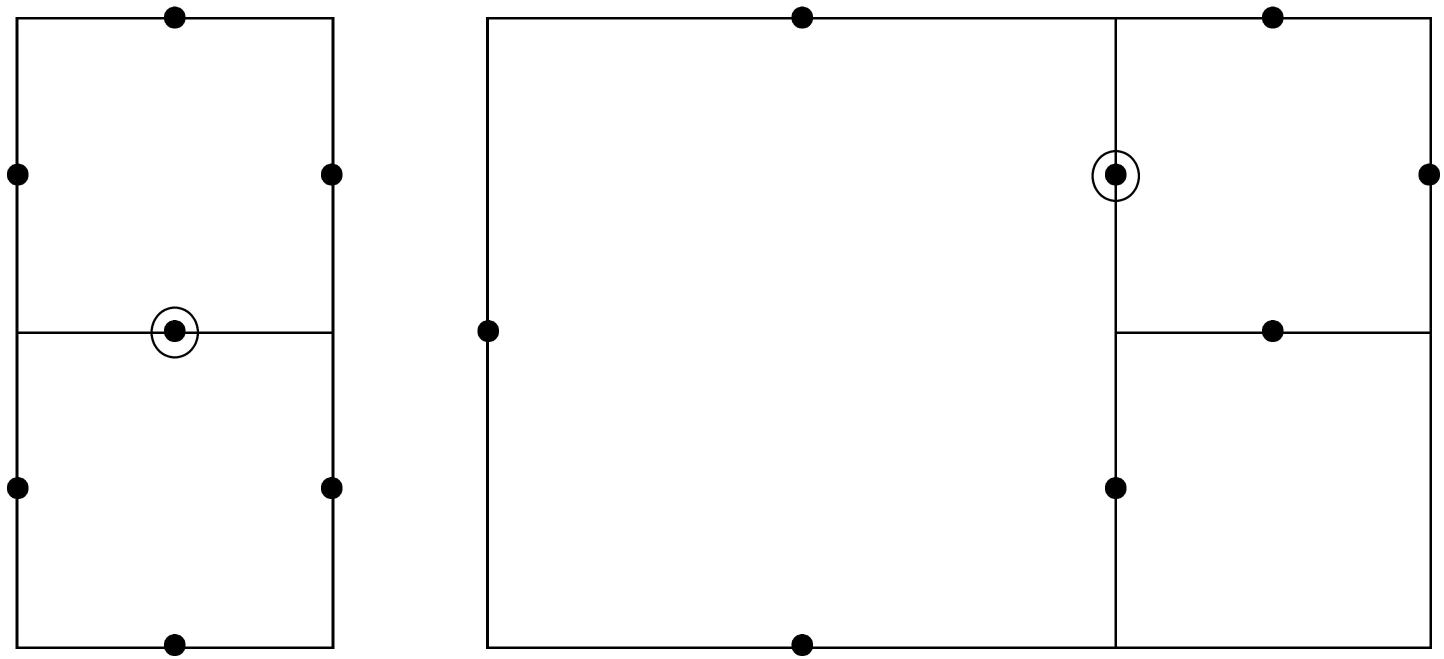

Numerical experiments (1/4)

The derived mimetic discretizations are exact for linear solutions.

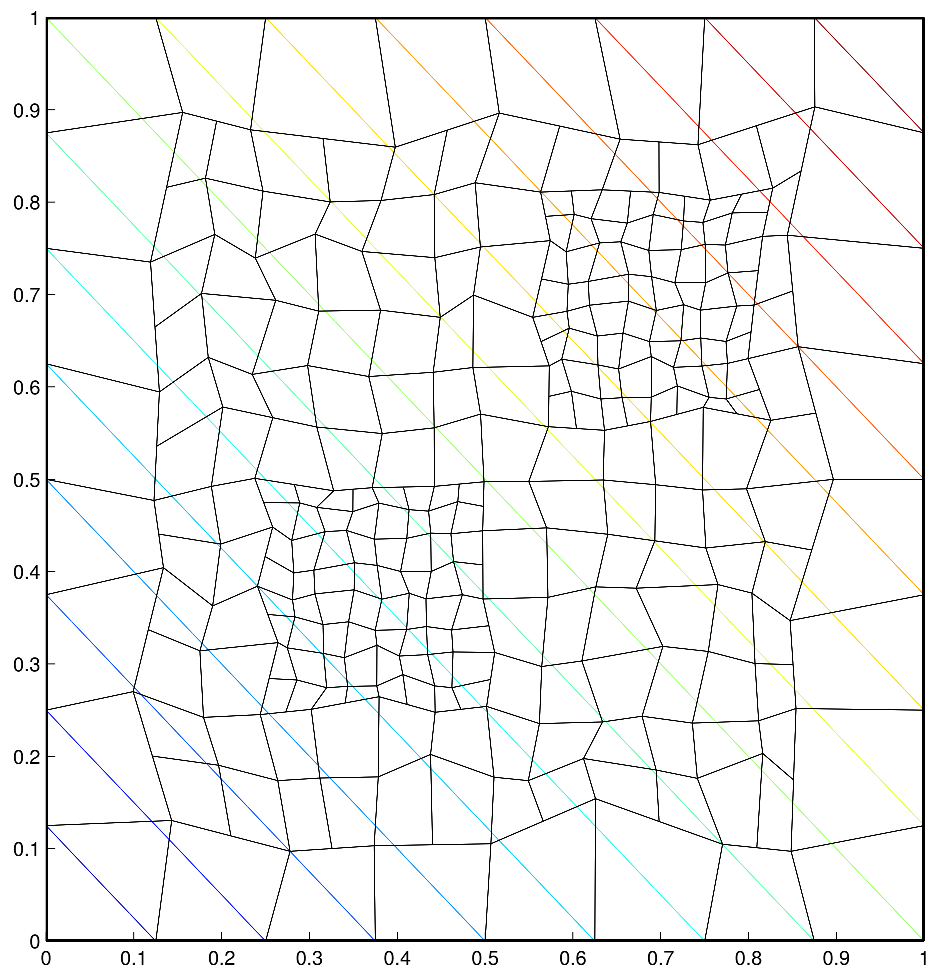

Numerical experiments (2/4)

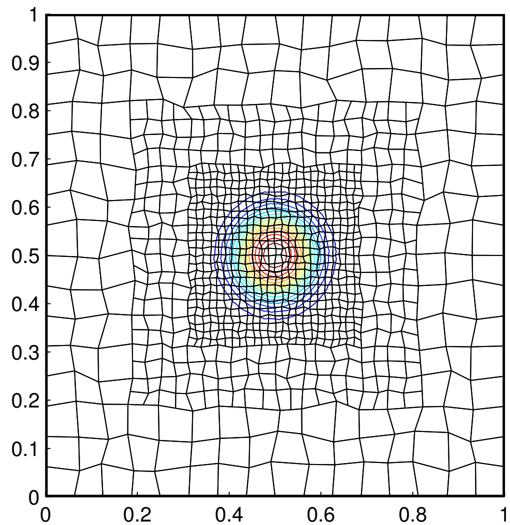

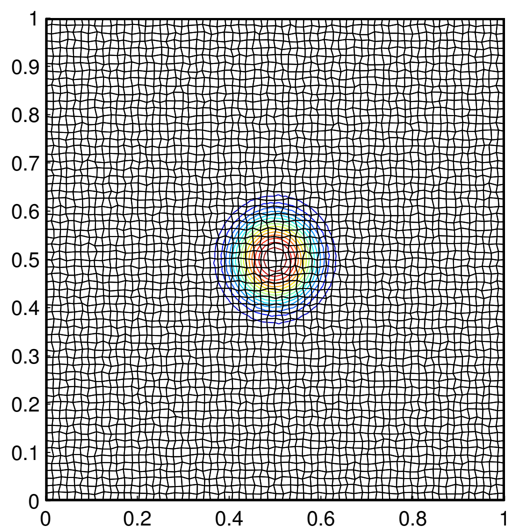

l	N	ε_p	$\varepsilon_{\boldsymbol{f}}$	#itr	CPU,s
	AMR grids				
0	256	7.00e-2	8.18e-2	12	0.05
1	556	1.64e-2	3.42e-2	15	0.14
2	988	3.74e-3	1.74e-2	16	0.28
3	3952	9.96e-4	7.57e-3	16	1.33
4	15808	2.40e-4	3.79e-3	17	6.21
	Uniform grids				
0	256	7.00e-2	8.18e-2	12	0.05
1	1024	1.79e-2	3.40e-2	13	0.27
2	4096	3.91e-3	1.62e-2	14	1.25
3	16384	9.44e-4	7.30e-3	15	5.58
4	65536	2.32e-4	3.76e-3	17	25.3

$$p(x,\,y) = 1 - \tanh\left(\frac{(x-0.5)^2 + (y-0.5)^2}{0.01}\right).$$

Numerical experiments (3/4)

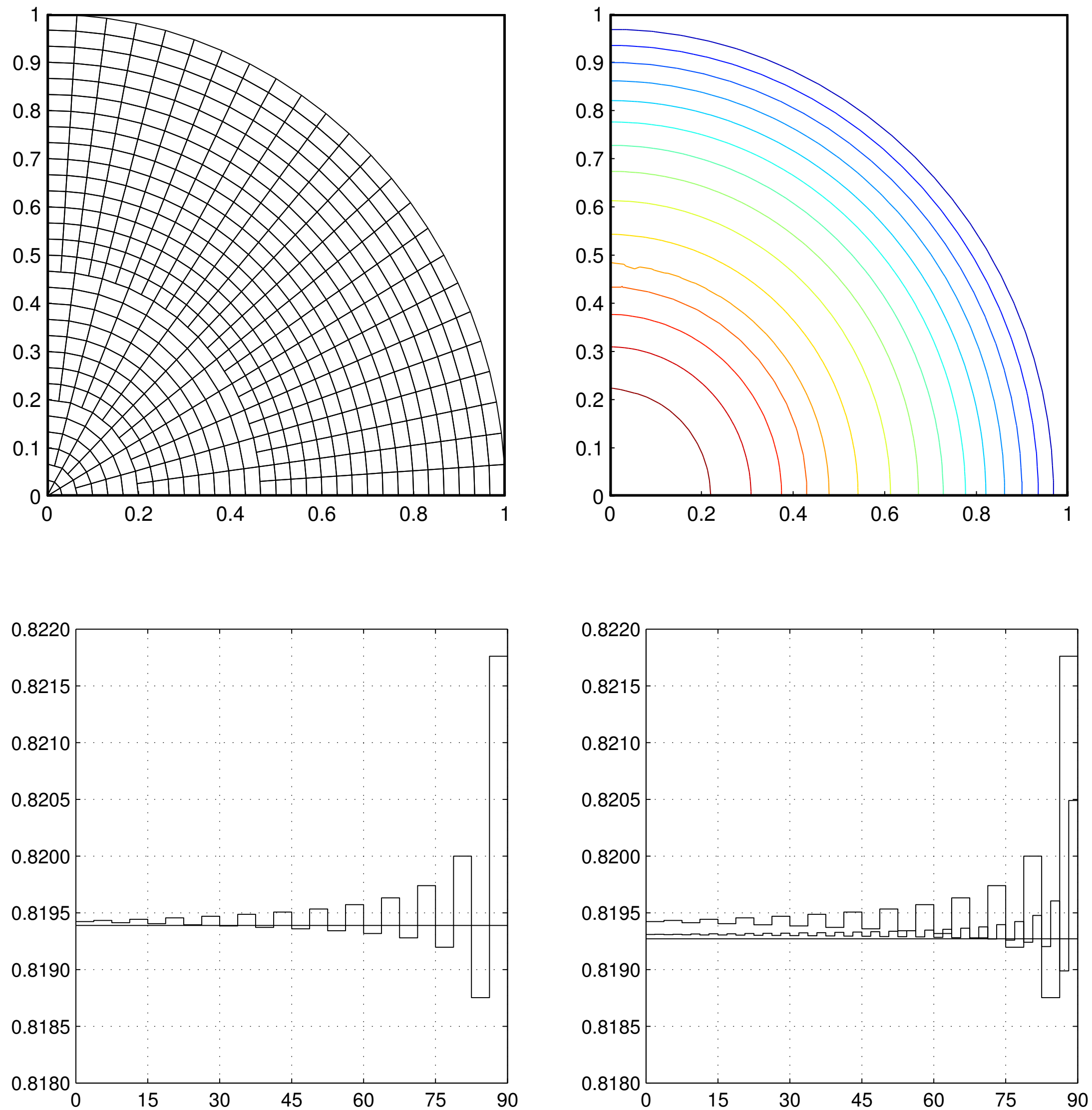

Spherically symmetric problem in $r - z$ coordinates with the exact solution:

$$p(R) = \frac{553}{640} - \frac{R^2}{6} - \frac{R^4}{20}$$

when $R < 0.5$ and

$$p(R) = \frac{101}{120} - \frac{R^2}{12} - \frac{R^4}{40}$$

when $0.5 < R < 1.$

Numerical experiments (4/4)

Let us consider the diffusion problem with strong material discontinuity

$$[\boldsymbol{K}] = 100 \quad \text{at} \quad \sqrt{(x-0.5)^2 + (y-0.5)^2} = 0.25.$$

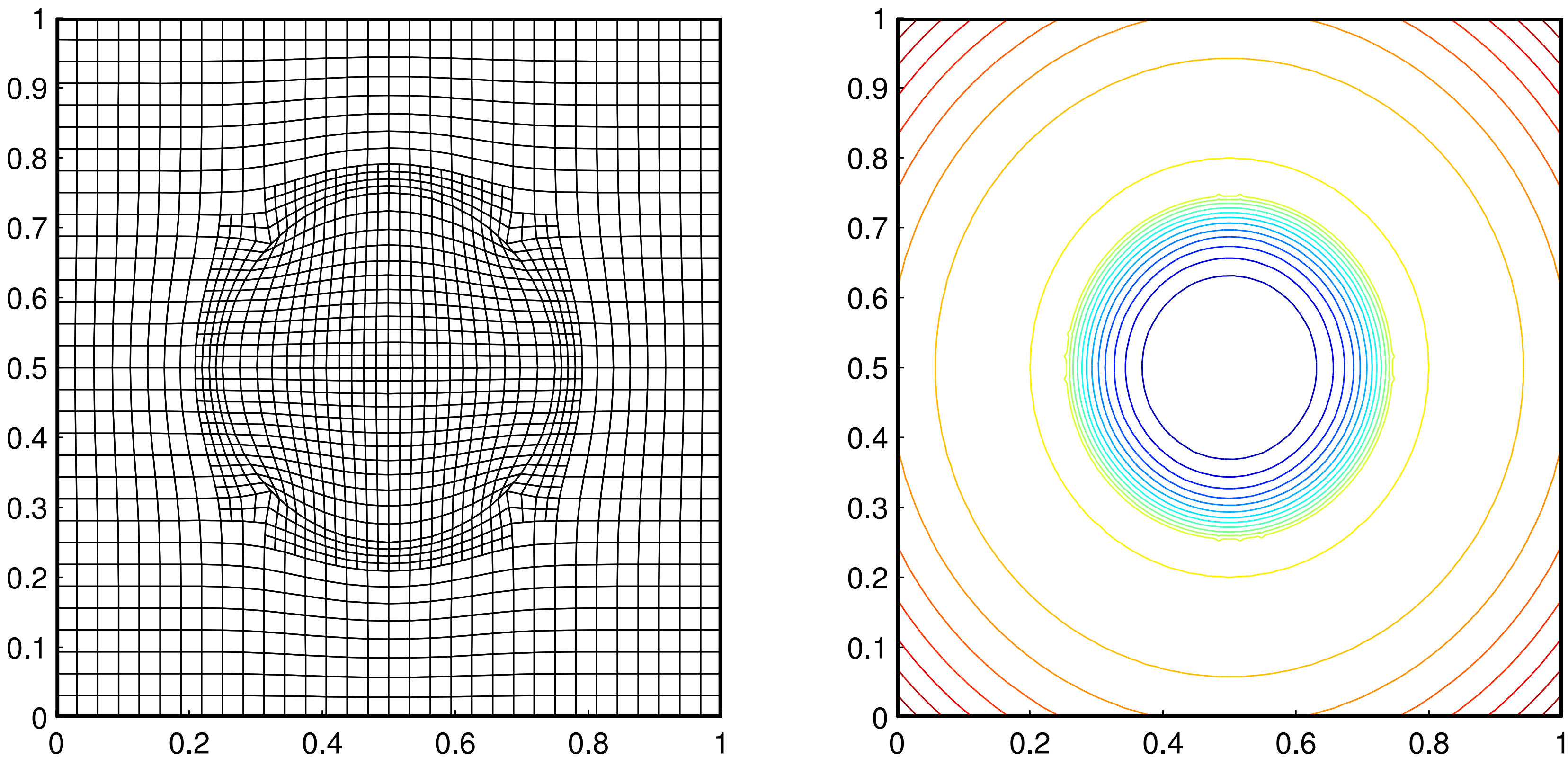

The locally fitted grids were generated by Shengtai Li (T-7).

SO and mixed FE methods (1/1)

- A connection of the SO method with a mixed-hybrid FE method can be used to proof convergence of mimetic discretizations.
- The numerical experiments with highly heterogenous diffusion coefficients have shown that the black-box multigrid method (AMG by K.Stüben and J.Ruge) is more robust in the case of SO discretizations.
- In the case of conformal quadrilateral meshes, the SO and FE methods result (asymptotically) in the same discretization errors; however, the FE method requires a very accurate quadrature rule for integrating Raviart-Thomas finite elements. The methods are identical when these finite elements are used to derive the quadrature rule $[f^d, g^d]_X$.

SO and FD methods (1/1)

In collaboration with M.Pernice (CCS-3), the SO method was compared with the FD method by R.Ewing, R.Lazarov, and P.Vassilevki (1991):

- the FD method works on rectangular locally refined grids;
- in the case of smooth solutions, the FD method results in larger error (left picture) on irregular grid interfaces:

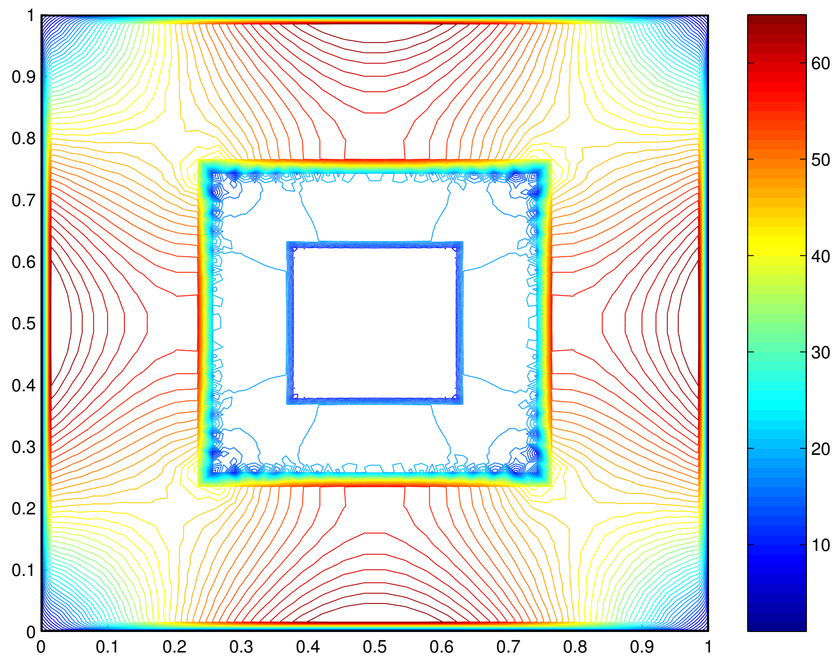

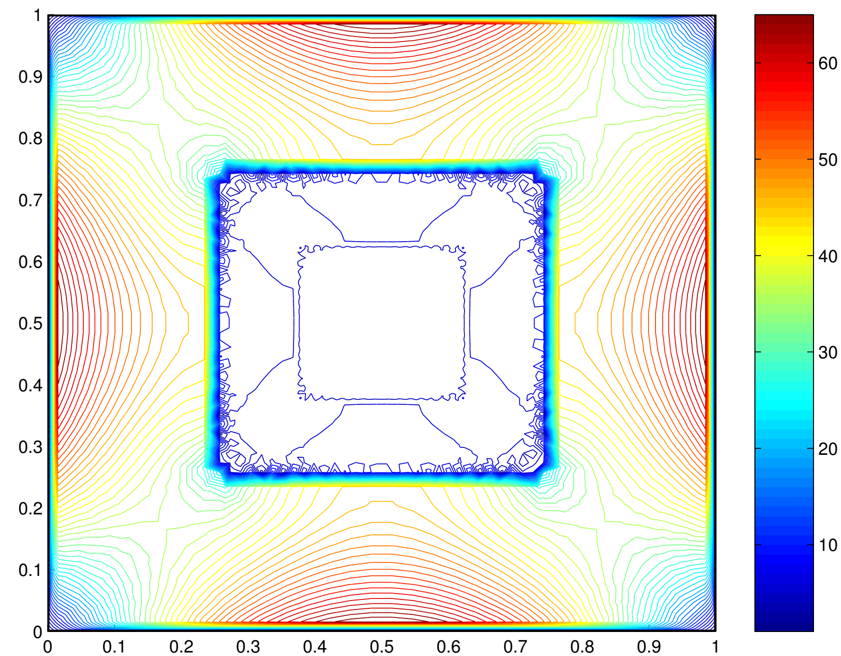

SO and CV methods (1/1)

The control-volume mixed FE method by T.Russell (2001):

- the method does not preserve the uniform flow on irregular grids;
- the principle difficulty is the scalar product in a space of fluxes.

The control-volume method on general polygonal meshes by T.Palmer (2001):

- the method is exact for linear solutions;
- the method results in non-symmetric matrices.

The SO method on general polygonal meshes (200?):

- the method is exact for linear solutions;
- the method results in symmetric positive definite matrices.

Conclusion

- the convergence of mimetic discretizations for the linear diffusion equation is optimal on locally refined meshes in both Cartesian and $r - z$ geometries (2nd order on smooth meshes but only 1st order for fluxes on random grids);
- the mimetic discretizations are closely connected with mixed-hybrid FE discretizations and more preferable than the discretizations based on CV or FD methods;
- a reduced system for interface intensities has the SPD coefficient matrix and can be efficiently solved with a PCG method;
- the symmetry breaking in the $r - z$ coordinate system has to be analysed.